

# Measuring Wear using Image Processing Techniques

M.B. de Rooij and D.J. Schipper  
University of Twente

## Abstract

*A new method of measuring wear, based on 3D measurement of the surface microgeometry and image processing techniques is introduced. The method is able to characterise wear of very wear resistant materials, with depths of wear tracks in the order of the roughness or less. The method will be introduced and some results will be presented.*

## 1 Introduction

Wear is mostly measured by measuring mass losses, measuring volume losses by measuring cross-sections of wear tracks or measuring displacements during the experiment. These classical methods, although relatively easy to perform, have several disadvantages:

- Measuring significant wear at tribologically interesting materials (mostly wear resistant materials) results in relatively long measuring times of the wear test to generate for example a mass difference that is measurable.
- Using these methods, it is only possible to get a global impression of the mass difference generated during a tribological experiment. In general, wear is not a global, but a local phenomena that has its origins at the microcontacts between both contacting bodies and, eventually, third body particles (for example wear debris) in the contact.
- The measured mass difference is not automatically the mass loss caused by wear processes. Besides mass loss caused by wear processes, in tribological contacts there may be mass addition caused by material transfer between the contacting bodies. The measured mass difference is the resulting mass difference caused by transfer and wear mechanisms.

This report is about an alternative wear measuring method based on image processing techniques. This way of measuring wear can be used to measure wear of very wear resistant materials. The method results in information about local differences at the surface, caused by wear and material transfer processes. The method is also able to separate the material added by material transfer processes from the material removed by wear processes.

## 2 Overview of the measuring method

The measuring method is shown schematically in figure 1.

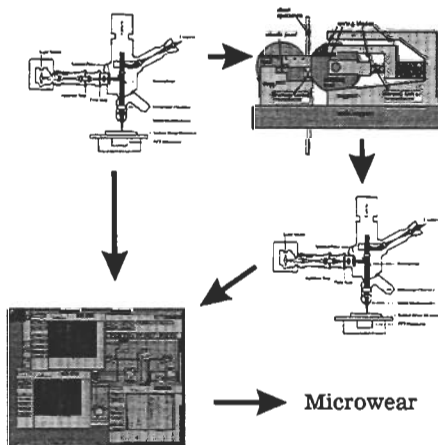


Figure 1: overview of the measuring method

First, measurements of the microgeometry are done with a 3D-interference microscope. Using, this instrument, it is possible to measure a square part of the sample with a height resolution of less than 1 nm. Then the wear test is performed on a tribological tester, in this case

a strip drawing device. After the wear test, the surface microgeometry is measured for the second time on, as accurate as possible, the same spot of the sample. To accomplish this, precise positioning tools are used. This information of the surface microgeometry obtained by both measurements, is processed by image processing software to obtain the difference image between both measurements of the microgeometry. This difference image gives local information about wear and material transfer. One of the main problems is matching of both surfaces, i.e. positioning the second image exactly over the first image. This is, besides subtraction of both surfaces, the main task of the image processing software.

### 3 Matching of the surfaces

In general, there are six degrees of freedom defining the position of a plane relative to another plane. To match two surfaces, all six possible transformations have to be defined. These six translations and rotations can be reduced to three in the following way: Using the 3D-interference microscope, all measurements are given relative to the least-square reference plane. By excluding the worn parts of the surface from the calculation of the reference plane, and using the same areas for the calculation of the reference plane of the measurement done before the wear test results in an equal least squares regression plane for both measurements. In this way three degrees of freedom remain: two translations and one rotation. Until now, these are found by searching corresponding points in the images with the human eye. The coordinates of the corresponding points give information about the translations and the rotation that have to be performed on one of the images to let them cover the same area: Two translations, in  $x$ - and  $y$  direction are given by the differences of the  $x$  and  $y$  coordinates of a reference point  $i$ .  $x$  and  $y$  are the 'source' coordinates, and  $x^*$  and  $y^*$  are the 'target' coordinates.

$$t_x = x_i^* - x_i \quad (1)$$

$$t_y = y_i^* - y_i \quad (2)$$

The absolute value of the rotation angle  $\phi$ , with point  $i$  as the center of rotation, can be calculated using the cosine rule:

$$z = \sqrt{(x_i^* - x_j^*)^2 + (y_i^* - y_j^*)^2} \quad (3)$$

$$b = \sqrt{(x_i^* - (x_j + t_x))^2 + (y_i^* - (y_j + t_y))^2} \quad (4)$$

$$c = \sqrt{((x_j + t_x) - x_j^*)^2 + ((y_j + t_y) - y_j^*)^2} \quad (5)$$

$$|\phi| = \arccos\left(\frac{a^2 + b^2 - c^2}{2ab}\right) \frac{360}{2\pi} \quad (6)$$

Using successively all corresponding points as center of rotation  $i$ , and, given a certain point  $i$ , calculating the angle of rotation  $\phi_{ij}$  necessary to overlap point  $j$  and  $j^*$  for all  $j$ , a matrix  $R$  containing angles of rotation can be constructed:

$$R = \begin{bmatrix} \phi_{1,1} & \phi_{1,2} & \dots & \phi_{1,n} \\ \phi_{2,1} & \dots & & \vdots \\ \vdots & & \phi_{n-1,n-1} & \phi_{n-1,n} \\ \phi_{n,1} & \dots & \phi_{n,n-1} & \phi_{n,n} \end{bmatrix} \quad (7)$$

Inspecting this matrix  $R$  gives some information about the accuracy of the visually found corresponding points. An inaccurate point  $i$  will be recognisable by the irregular columns and rows  $i$  in the matrix. The actual angle of rotation  $\phi_f$  is determined from this matrix by choosing a reference point  $i$  which has the least spread in the calculated angles  $\phi$ . Leaving the inaccurate points, and averaging the angles  $\phi$ , of column (or row)  $i$  gives the final angle of rotation  $\phi_f$  that is used to actually rotate the image. Experimental investigation in the image processing software gives the + or - sign of the angle of rotation  $\phi_f$ . In this way the inaccurate points can be left out of the calculations, and a more accurate angle of rotation can be calculated, using all the available information of the accurate corresponding points. In practice, the angle of rotation can be calculated with an accuracy of tens of degrees or sometimes hundreds of degrees, depending on the contrast of the image, and therefore on the microgeometry of the surface. This is of a great influence on the accuracy of the corresponding points found.

### 4 Some Results

As an example, the results based on the measured microgeometry of a TiN coated sample in the middle of the contact area, measured before and after a wear test will be presented. Two experiments were performed on the sample: A lubricated experiment followed by an unlubricated experiment. This means that from the chosen

spot three measurements in total were made: One measurement before the lubricated experiment, one measurement between the lubricated and the unlubricated experiment and one measurement after the unlubricated experiment. No additional operations, except the interpolation of missing points in the measurements of the microgeometry from their neighbouring points, the transformations and subtraction of the images, were performed on the images shown. Contour plots of the measurements taken on this spot are shown in figures 2, 3 and 4. The height values shown in these figures are ranged from  $-0.3\mu\text{m}$  to  $0.08\mu\text{m}$ . The measured area is  $1.35\text{ mm} \times 1.75\text{ mm}$ . In this area, the microgeometry is measured on  $304 \times 228$  points. The difference between these surfaces, after performing the two translations and the rotation on one of the images, is shown in figure 5. This image is scaled from  $-0.05\mu\text{m}$  to  $0.05\mu\text{m}$ . The applied translation in  $x$ -direction, determined by equation (1) is 5 pixels, in  $y$ -direction, determined by equation (2) is 8 pixels. The rotation angle, determined by equations (3) to (7) is  $1.55^\circ$  (clockwise). These transformations are performed on the image, shown in figure 3. As can be seen in figure 5, the surface of the TiN coating is not worn over the whole surface, but the coating surface has a grooved appearance. The depth of the wear tracks is approximately 50 nm. This depth does not vary significantly over the length of the wear track (see figure 6), despite the relatively high height differences of the surface. The beginning of the wear track is a deep 'hole'. Some of these holes were already existent before the wear test. These holes have a depth of 200-250 nm according to the surface microgeometry measurement. The holes are not deep enough to reach the surface of the substrate. These holes seem to be the starting points of the wear tracks. Archard's K-value can in principle be determined by intergrating over the surface, and only taking into account the negative points. Comparison the measurement before the unlubricated experiment and after the unlubricated experiment (not shown here) shows that the unlubricated experiment does not create new wear tracks in the surface. It seems to be a continuation of already existent wear tracks, formed during the preceding lubricated experiment. The wear tracks all have an almost equal width of  $10\mu\text{m}$ . This value is not very accurate, because of resolution of the measurement system of  $5.7 \times 5.8\mu\text{m}$  with the used

magnification.

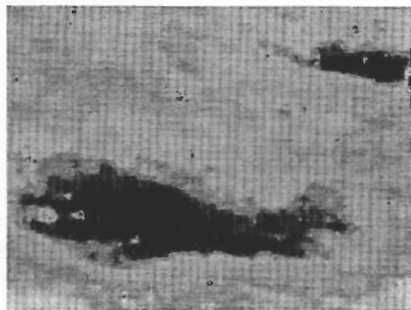


Figure 2: 2D-view of spot 2 on sample TiN22 before the lubricated experiment

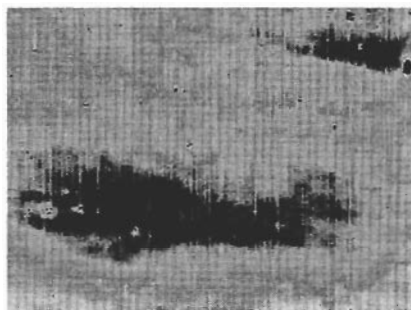


Figure 3: 2D-view of spot 2 on sample TiN 22 after the lubricated experiment (and before the unlubricated experiment)

## 5 Conclusions

- The method is able to characterise wear on the level of the microgeometry.
- Using this method, it is possible to distinct between material transferred to the surface and material worn off the surface, if the two mechanisms do not occur simultaneously on the same spot.
- Studying wear using the method gives extra insight into the wear mechanisms in the contact.

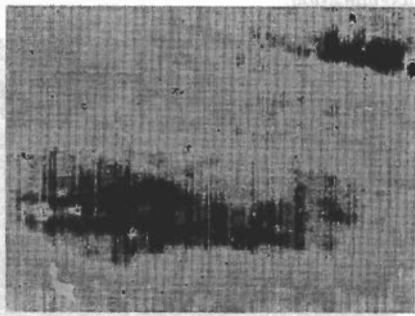


Figure 4: 2D-view of spot 2 on sample TiN 22 after the unlubricated experiment



Figure 5: 2D-view of the changes in the surface, caused by the lubricated experiment

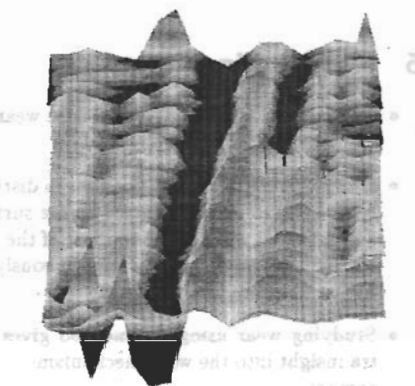


Figure 6: The wear track has equal depth over his whole length

Figure 4 shows the surface of spot 2 on sample TiN 22 after the unlubricated experiment. The surface is dark and irregularly shaped, indicating significant wear and damage. Figure 5 shows the surface of the same spot after the lubricated experiment. The surface is much smoother and shows a series of vertical, parallel lines, indicating that the lubrication has significantly reduced the wear and damage. Figure 6 is a 3D surface plot of the wear track, showing that the wear track has a consistent depth across its entire length. This indicates that the lubrication has effectively reduced the wear and damage to a uniform level.